World Journal of Advanced Engineering Technology and Sciences
eISSN: 2582-8266
Cross Ref DOI: 10.30574/wjaets
Journal homepage: https://wjaets.com/

(RESEARCH ARTICLE)

Check for updates

Geophysical investigation of crustal structural framework of Ilesha, southwestern Nigeria

Emmanuel Rotimi Olafisoye [1,*], Adediran Olanrewaju Adegoke [1] and Olufemi Adigun Alagbe [2]

[1] *Department of Physical Sciences, Olusegun Agagu University of Science and Technology, Okitipupa, Nigeria.*
[2] *Department of Applied Geophysics, Federal University of Technology, Akure, Nigeria.*

World Journal of Advanced Engineering Technology and Sciences, 2022, 05(02), 123–135

Publication history: Received on 14 March 2022; revised on 21 April 2022; accepted on 23 April 2022

Article DOI: https://doi.org/10.30574/wjaets.2022.5.2.0052

Abstract

The interpretation of the aeromagnetic dataset of Ilesha southwestern Nigeria has been carried out to reveal possible future earthquake hazard as well as establish the groundwater potential of the area. The edge detection methods involving the analytical signal amplitude, the total horizontal derivative, the first vertical derivative and the 3D Euler deconvolution were performed on the residual magnetic intensity anomalies to identify the linear structural discontinuities associated with lithological boundaries/ faults in the area. The upward continuation filter and depth estimation procedures of source parameter imaging and radially averaged power spectrum were applied to the residual magnetic intensity data to map geological structures such as faults as well as determine the depth to crystalline basement rocks in the area. The obtained lineaments observed to trend predominantly towards the NE-SW direction indicative of Pan African Orogeny, suggest possible high yield groundwater aquifer zones. The upward continuation filtered maps showed evidence of deep-lying faults to depth beyond 2 km. The 3D Euler deconvolution plots and spectral analysis revealed depth to magnetic sources ranging from 55 m to 345 m and 13 m to 250 m, respectively. The delineated structural discontinuities in the study area revealed stress history similar to Ifewara-Zungeru fault network, suggestive of possible future earthquake occurrence in the area. It is however recommended that further geophysical studies should involve electrical method to establish the groundwater potential as well as the stability of the basement underlying the area.

Keywords: Aeromagnetic; Anomaly; Edge detection; Euler deconvolution; Lithology; Source parameter imaging

1. Introduction

Aeromagnetic survey is suitable in delineating the lithostructural settings of the crystalline basement rocks as it readily unveils the crustal stability as well as zones of mineralization. In circumstances where a well-documented geological map is unavailable, a thorough aeromagnetic map is essential [1]. The main goal of magnetic surveying is to look into subsurface structures based on variations in the detected magnetic field caused by variances in the magnetic properties of the underlying rocks. The magnetic field anomaly signature may be associated with local mineralisation, or could be attributed to cases of structurally controlled hydrocarbon deposits. The magnetic prospecting method is a versatile procedure. Hence, it is commonly used in exploration programs [2].

Magnetic susceptibility is a variable function as it depends majorly on the ferromagnetic contents in various rock types underlying an area. In other to determine the variation in earth's magnetic field, there is need to carry out a comprehensive and detailed magnetic investigation, which can be achieved through ground, airborne or marine survey [3] depending on factors such as accessibility and area extent. The geology of the Ilesha Schist belt in southern Nigeria is complex, with two major fracture zones, the Iwaraja fault in the east and the Ifewara fault in the west, affecting its

* Corresponding author: Emmanuel Rotimi Olafisoye
Department of Physical Sciences, Olusegun Agagu University of Science and Technology, Okitipupa, Nigeria.

structural integrity [4,5,6]. The Ifewara fault runs from Ijebu Ode in the south to the Niger River valley south of Lafiagi in the north [7]. Previous research has revealed a link between the fracture and the Atlantic Ocean's notable Okitipupa Ridge [8,7]. It extends north-eastwards as the Zungeru mylonites beyond the Nupe Basin [9].

In this current study, high resolution airborne magnetic data was used in the investigation of the litho-structural stability of the study area as knowledge relating to the crustal deformation of the area will be crucial in groundwater development as well as mitigating possible future earthquake occurrence. Comparative study of edge detection methods involving analytical signal amplitude, total horizontal derivative, first vertical derivative, tilt derivative and 3D Euler deconvolution was carried out to reveal the orientation and distribution of structures associated with faults and lineament intersections within the area.

2. Geological settings

The study area is geologically underlain by the Ilesha Schist belt of Southwestern Nigeria bounded within Longitudes 4^{O} 30' to 4^{O} 45' E and Latitudes 7^{O} 30' to 7^{O} 45' N (Fig. 1). This area falls within the Precambrian rocks from the Archaean to Lower Proterozoic Basement Complex in Southwestern Nigeria [8,10,11].

According to Ferre et al. [12], the area is classified into two major terranes comprising the eastern and the western sections. The narrow, sediment-dominated north-south trending, low-grade schist imprinted western terrane composes primarily of migmatite gneiss basement intruded by Pan African granitic plutons [13,14]. On a regional scale, the area has been recognized as having steeply dipping Neoproterozoic shear zones that predominantly trend northeast-southwest [15,16]. As a result of intense shearing and fracturing, the rocks of the Ilesha Schist belt are banded, foliated, and show signs of polydeformation [9,17,15,18].

The rock types consisting of migmatite, porphyritic granite, amphibolites, amphibolite schist, quartz schists and quartzite underlying the study area is intruded by granite metamorphosed into gneisses [7]. The Nigerian Schist belt have been studied and adequately documented and it is known to be associated with gold mineralisation [19].

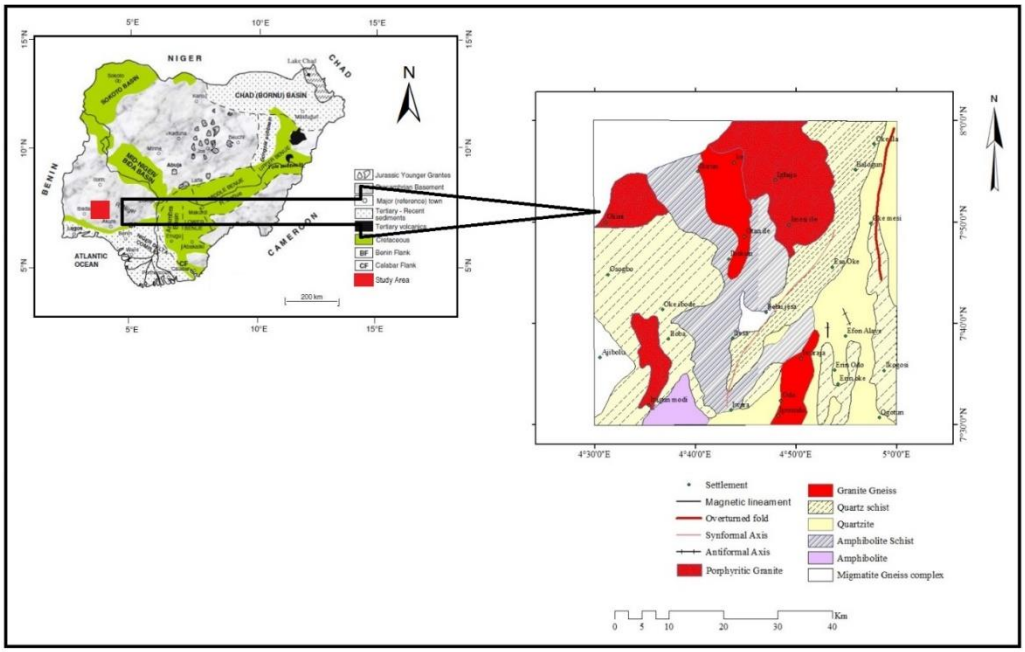

Figure 1 Geological map of Nigeria showing the study area (modified after Obaje, 2009)

3. Methodology

The total magnetic intensity map was created using aeromagnetic data obtained from the Nigeria Geological Survey Agency (NGSA) and gridded at 100 m spacing using the minimum curvature gridding method. The data was measured at intervals of approximately 7 m with a nominal flight height of 80 m above the terrain. The survey used a 500 m flight line spacing and a 2 km tie line spacing, with the flight line trending northwest–southeast and the tie lines trending

northeast–southwest. The dataset was subsequently processed using geosoft oasis montaj, arcGIS 10.3 and rockworks 15 software applications.

The total magnetic intensity map was subjected to a reduction-to-equator procedure for positioning of the individual anomalies over their associated magnetic sources. Because the geophysical survey was conducted in a low latitude area, this approach simplifies interpretation by changing magnetic data acquired at varied magnetic field inclinations to zero inducing field inclination [20]. The reduction-to-equator map was upward continued to 200 m to remove high frequency signals from sources on or near the ground surface. The resulting map was further filtered by the removal of regional field; corresponding to an upward continued height of 80 km. Hence the residual magnetic intensity map was produced after the regional field was removed.

Edge detection methods involving first vertical derivative, analytical signal amplitude, total horizontal derivative and Euler deconvolution, were subsequently applied to the residual magnetic intensity map to improve the subsurface geological structures and lithological boundaries associated with fractures, faults and contacts in the study area.

Upward continued filter was also performed to delineate deep seated as well as shallow lying faults in the area. This filter transforms magnetic data to that which would be observed at different depths below the actual observation level. This filtering method suppresses high frequency anomalies, thereby attenuating the effect of near surface magnetic sources relative to deeper sources [21]. It can be expressed mathematically as:

$$L(r) = e^{-hr}, \tag{1}$$

The expression for r is given as

$$r = \sqrt{u^2 + v^2} = 2\pi k. \tag{2}$$

where h is the new height, u and v are the Fourier domain wave numbers, and k is cycles/unit.

The first vertical derivative filter improves the short wavelength responses in the data by eliminating the long wavelength anomalies. It is applied because it is the least susceptible to noise when compared with the higher order vertical derivatives [20].

The amplitude of the analytical signal is the square root of the squared summation of the vertical and horizontal derivatives of the magnetic field, as expressed by MacLeod et al. [22] in equation (3).

$$ASA = \sqrt{\left(\frac{\partial M}{\partial x}\right)^2 + \left(\frac{\partial M}{\partial y}\right)^2 + \left(\frac{\partial M}{\partial z}\right)^2}. \tag{3}$$

The analytic signal technique is independent of magnetization direction [23], however it peaks over the edges of source bodies. The source edge positions can also be depicted using this magnetic data augmentation method [20].

Total horizontal derivative method is extensively used for the estimation of boundaries associated with shallow magnetic bodies. This filtering technique which shows low sensitivity to noise has high amplitude over the edge of the magnetic sources. The total horizontal derivative can be determined by the equation below:

$$THDR = \sqrt{\left(\frac{\partial M}{\partial x}\right)^2 + \left(\frac{\partial M}{\partial y}\right)^2}. \tag{4}$$

Where $\frac{\partial M}{\partial x}$ and $\frac{\partial M}{\partial y}$ are the two horizontal derivatives of the observed field (M).

Euler deconvolution was further employed for the delineation of magnetic source geometry, location and depth. As a result, it is a boundary finding and depth estimation technique. The Euler's homogeneity equation, as described by Reid et al. [24], will be

$$(x - x_o)\frac{\partial M}{\partial x} \rightarrow +(y - y_o)\frac{\partial M}{\partial y} + (z - z_o)\frac{\partial M}{\partial z} = N(B - M). \tag{5}$$

if (xo, yo, zo) is the location of a magnetic source and the total field (M) measured at a point (x, y, z) has a regional value of B. The structural index value N is determined by the magnetic source geometry, and for contact, sill/dike/fault, pipe/horizontal or sphere, it can be indicated as 0, 1, 2, or 3, respectively. According to Thompson [25] and Reid et al. [24], a correct N causes the Euler solutions to cluster tightly around the geologic structure of interest.

Spectral analysis was also applied to estimate the depth to magnetic sources through the application of Fast Fourier Transform approach [26]. It is a function of wavelengths in both the x and y directions. The windowed grid is processed to make its edges periodic. Lee [27] defined the Fourier transform f(μ,γ) of a periodic function f(x,y) as:

$$f(\mu\gamma) = \int_{-\infty}^{+\infty}\int_{-\infty}^{+\infty} f(x,y)\cdot e^{-i(\mu x+\gamma y)}dx\cdot dy. \quad (6)$$

where (x) and (y) denote the spatial coordinates in the x and y directions, respectively.

μ and γ indicate the angular frequencies in the x and y directions, respectively.

The source parameter imaging [28,29] or local wavenumber approach [30] uses the complex analytic signal concept to calculate source parameters from gridded magnetic data. Because this method necessitates the computation of first and second order derivatives, it is prone to noise and interference effects [31]. As a result, the peaks of the local wavenumber establish the inverse of depth for vertical contacts. Hence, the depth can be computed using the expression:

$$\text{Depth} = \frac{1}{K_{max}}, \quad (7)$$

Where K_{max} represents the peak value of the local wavenumber K above the steep source. The wavenumber is therefore calculated using the formula:

$$K_{max} = \sqrt{\left(\frac{\partial \text{Tilt}}{\partial x}\right)^2 + \left(\frac{\partial \text{Tilt}}{\partial y}\right)^2}. \quad (8)$$

In this study, the depth to anomalous causative bodies and the mapping of the basement topography were determined using depth estimation methods.

4. Results and discussion

4.1. Total magnetic intensity map

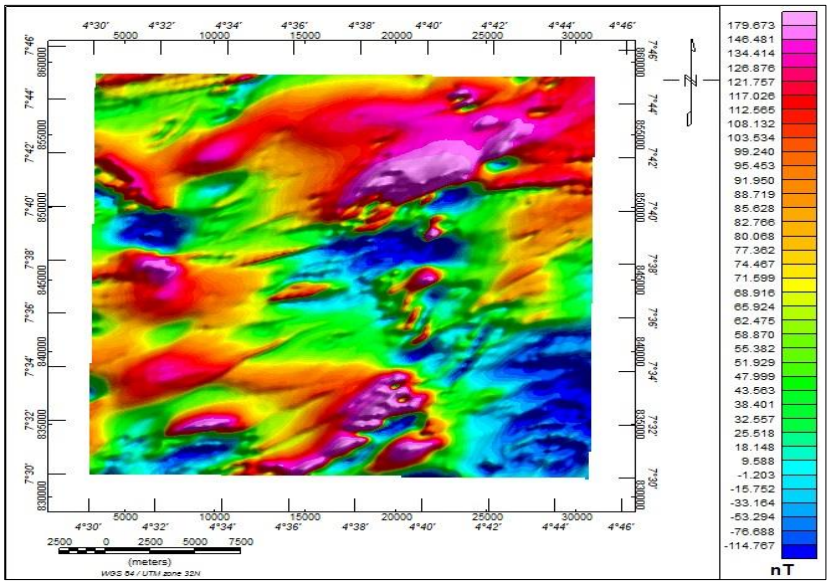

Figure 2 Total magnetic intensity map of the study area

The total magnetic intensity map indicated in Fig. 2, produced from the aeromagnetic data sheet of Ilesha, revealed changes in the study area's magnetic field intensity. The presence of distinct magnetic rocks with differing mineral compositions at varying depths in the subsurface could be responsible for the difference in detected magnetic anomalies. The magnetic field intensity amplitude ranged between -115 nT and 180 nT, indicating linear discontinuities of anomalies mostly oriented northeast-southwest (Fig. 2). The short wavelength anomalies depicted in the area correspond to near-surface magnetic outcrops while long wavelength revealed deep-seated basement rocks.

4.2. Reduction to equator map

The total magnetic intensity data was subjected to reduction to equator filtering with computed inclination and declination values of 8.41° and-1.4°, respectively. Sequel to the application of the filter, the amplitudes of the magnetic anomalies was observed to reduce from its initial minimum and maximum values to -92 nT and 172 nT, respectively as indicated in the reduced to equator map indicating slight variation from the total magnetic intensity anomalies. The resulting filtered map (Fig. 3) with anomalies better positioned above the causative bodies was subsequently upward continued to 200 m to suppress high frequency responses associated with near-surface noise in the data.

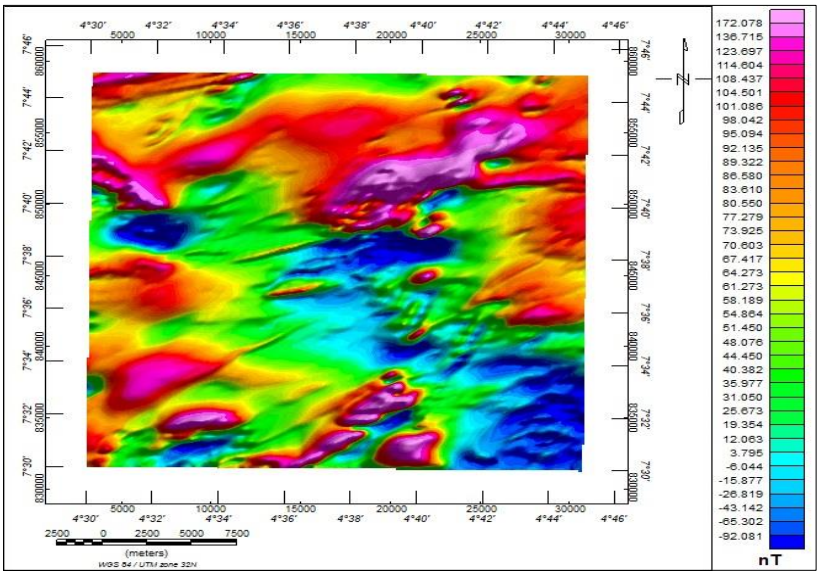

Figure 3 Reduced to equator map of the study area

4.3. Residual magnetic intensity map

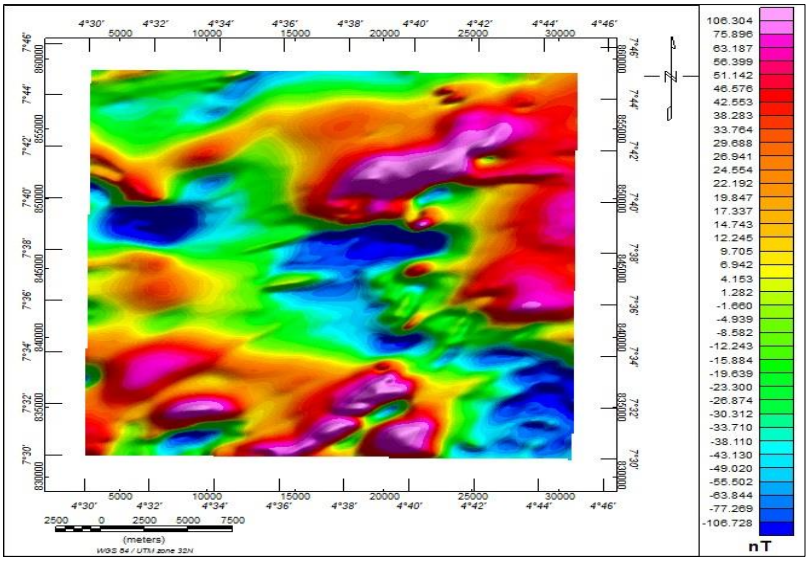

Figure 4 Residual magnetic intensity map of the study area

The near-surface noise filtered map was upward continued to a depth of 80 km to produce the regional field map of the study area. The resulting field map was subsequently subtracted from the former filtered map to reveal the residual magnetic anomalies associated with shallow lying magnetic events. The residual magnetic intensity map (Fig. 4) showed linear anomalies with varying magnetic susceptibility contrasts trending predominantly in the NE-SW direction within the study area similar to the total magnetic anomalies.

4.4. First vertical derivative

The residual magnetic intensity map was subjected to the first vertical derivative (FVD) filter to emphasize source edge locations by suppressing long wavelength anomalies (deep-lying magnetic features) within the study area. The resulting map (Fig. 5) clearly emphasized short wavelength responses indicative of shallow geological features within the study area; characteristic of crystalline basement complex rocks.

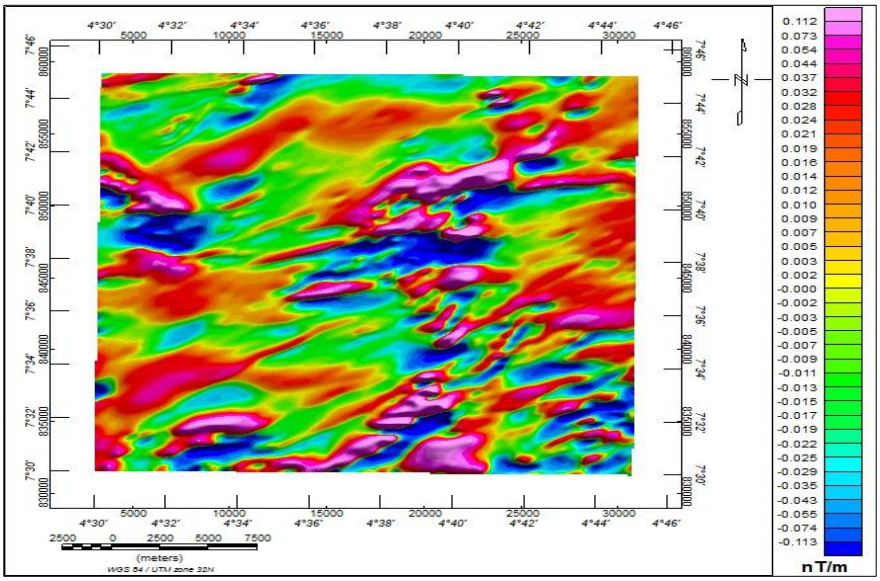

Figure 5 First vertical derivative map of the study area

4.5. Analytical signal amplitude map

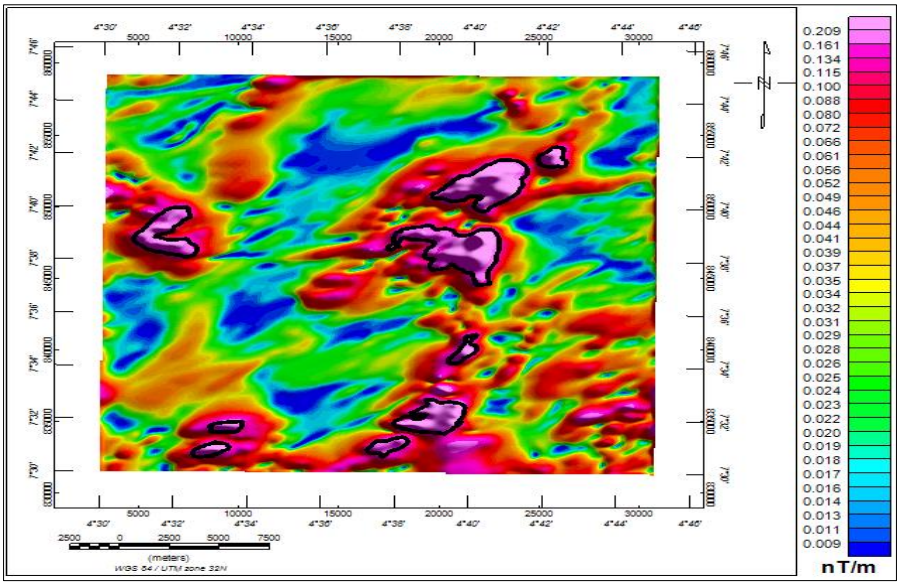

Figure 6 Analytic signal amplitude of the study area

The analytical signal amplitude (ASA) map of the residual magnetic anomalies is as indicated in Fig. 6. The magnitude of analytic signal delineates lithological boundaries between magnetic bodies; indicating geologic structural complexity in the crystalline basement fabrics. The analytical signal amplitude reveal continuous, thin, and straight peaking anomalies over the source edges in the study area

4.6. Depth estimation

4.6.1. Euler deconvolution

The plot of the 3D Euler Deconvolution (ED) obtained at structural indices of 0 and 1 gave the best linear clustering around some prominent geologic features interpreted as faults or lithological contacts within the study area (Fig. 7). The source edge locations depicted by the clustered Euler solutions were also identified on the analytical signal amplitude filtered map (Fig. 6).

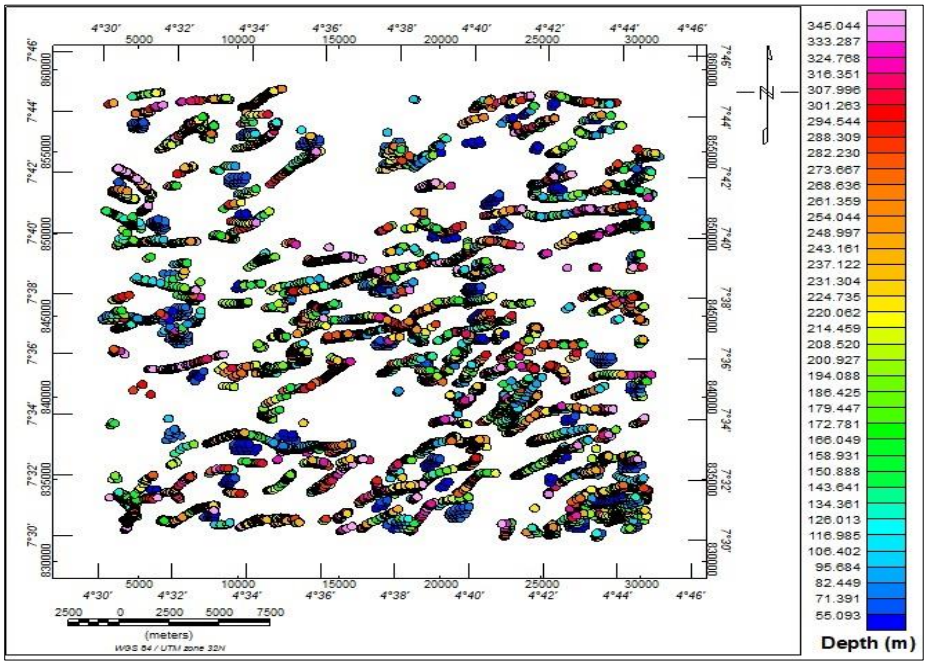

Figure 7 Plot of solutions of Euler deconvolution using structural index of 0 and 1

4.6.2. Spectral analysis

Spectral analysis was also performed on the residual magnetic anomalies to delineate depth to magnetic sources using the power spectrum method. This method is a well-known approach for estimating the depths of magnetic bedrocks underlying the study area. The computed depths as shown in Fig. 8 ranged between 13 m and 250 m and correlated well with the estimated depth for the 3D Euler deconvolution plots – 55 m to 345 m; for near-surface and deep magnetic sources, respectively.

Table 1 Depth estimation from spectral analysis

Spectra Blocks	Eastings		Northings		Depth (km)		
	$X_{minimum}$	$X_{maximum}$	$Y_{minimum}$	$Y_{maximum}$	Shallow	Intermediate	Deep
1	3023.25	19972.76	845003.47	859276.75	0.022	0.05	0.25
2	19972.76	30915.61	845003.47	859217.28	0.018	0.034	0.092
3	3082.72	19972.76	831324.92	845062.95	0.019	0.037	0.124
4	19913.29	30915.61	831324.92	845062.95	0.013	0.031	0.081

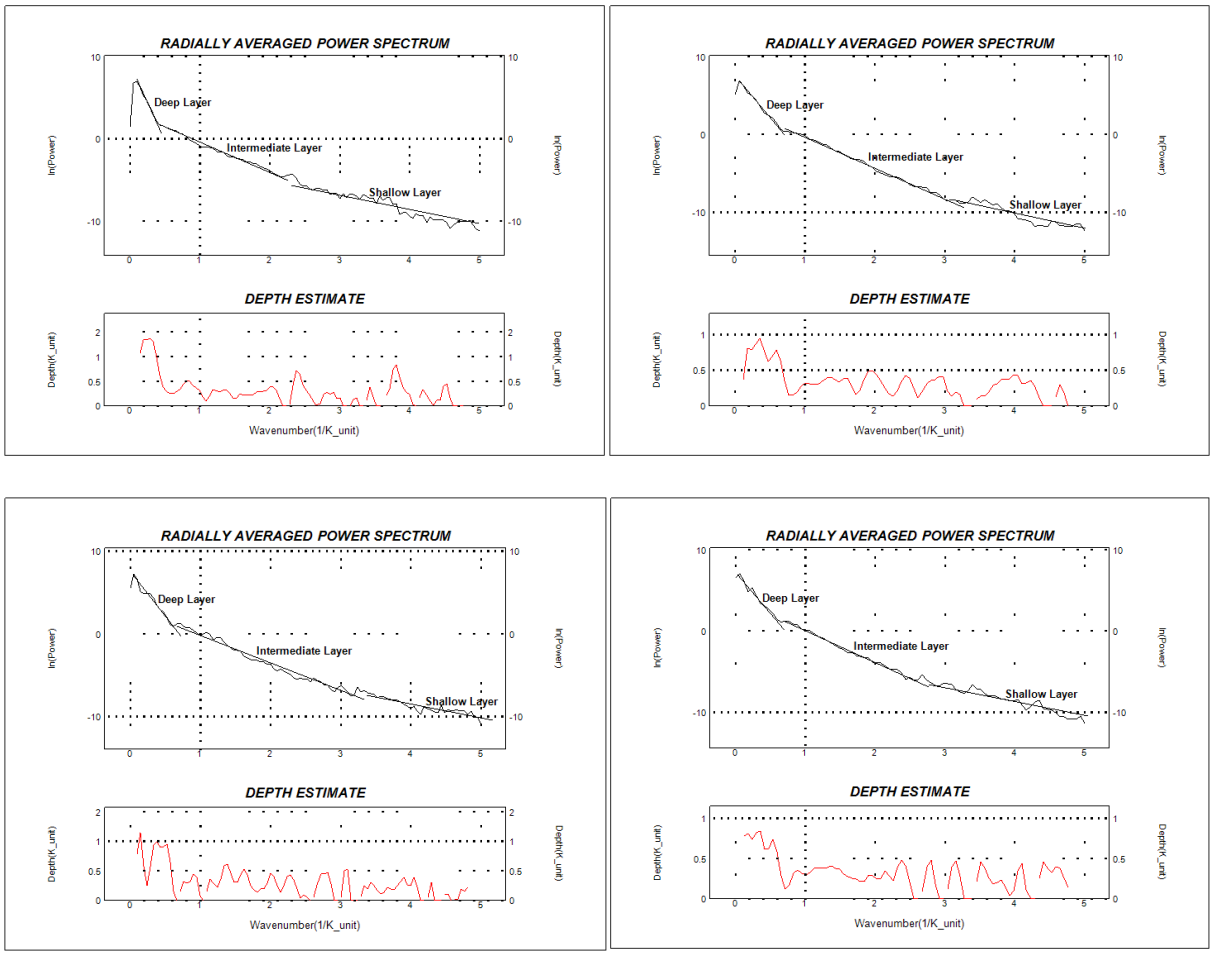

Figure 8 Radially averaged power spectrum estimate of depth to magnetic sources

4.6.3. Source parameter imaging

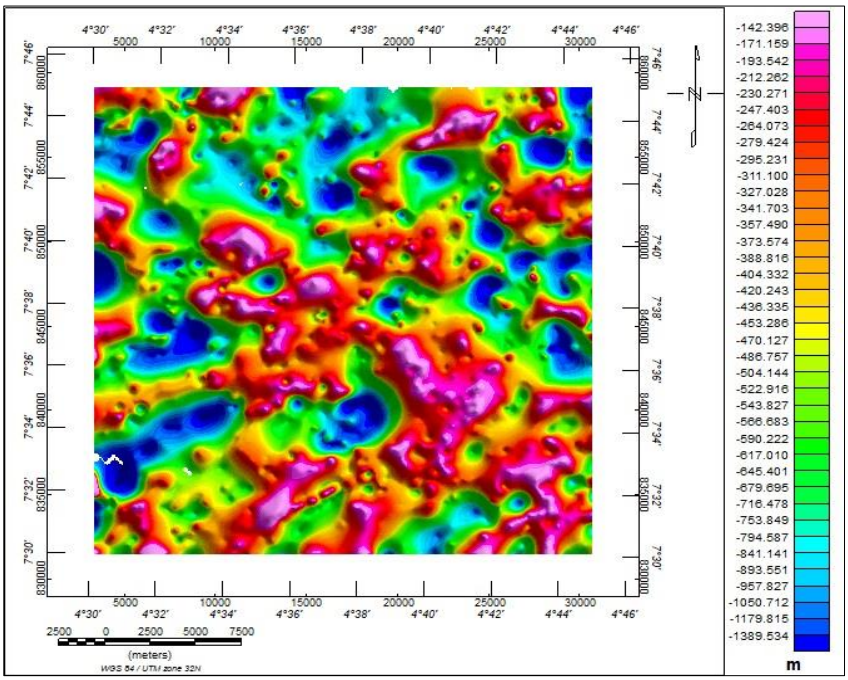

Figure 9 Source parameter imaging map of the study area

The source parameter imaging map which depicts variations in the overburden thickness in the study area revealed the prevalence of shallow lying magnetic bodies (Fig. 9). However, deep lying crystalline basement rocks can also be observed. Hence, the depth to basement ranged between 142 m and 1390 m as indicated in Fig. 9.

4.7. Structural map

4.7.1. Upward continuation maps

These filtered maps were produced from the transformation of the residual magnetic intensity anomalies to upward continued heights of 200 m, 500 m, 1000 m and 2000 m, respectively, above flight line elevation. In the study, geologic structures associated with faults were delineated from the upward continuation maps as presented in Fig. 10. The amplitude of the magnetic anomalies of the enclosed portions of the upward continuation maps was observed to decrease from a height of 200 m to 2000 m; indicative of faulted basement complex rocks at the subsurface within the study area.

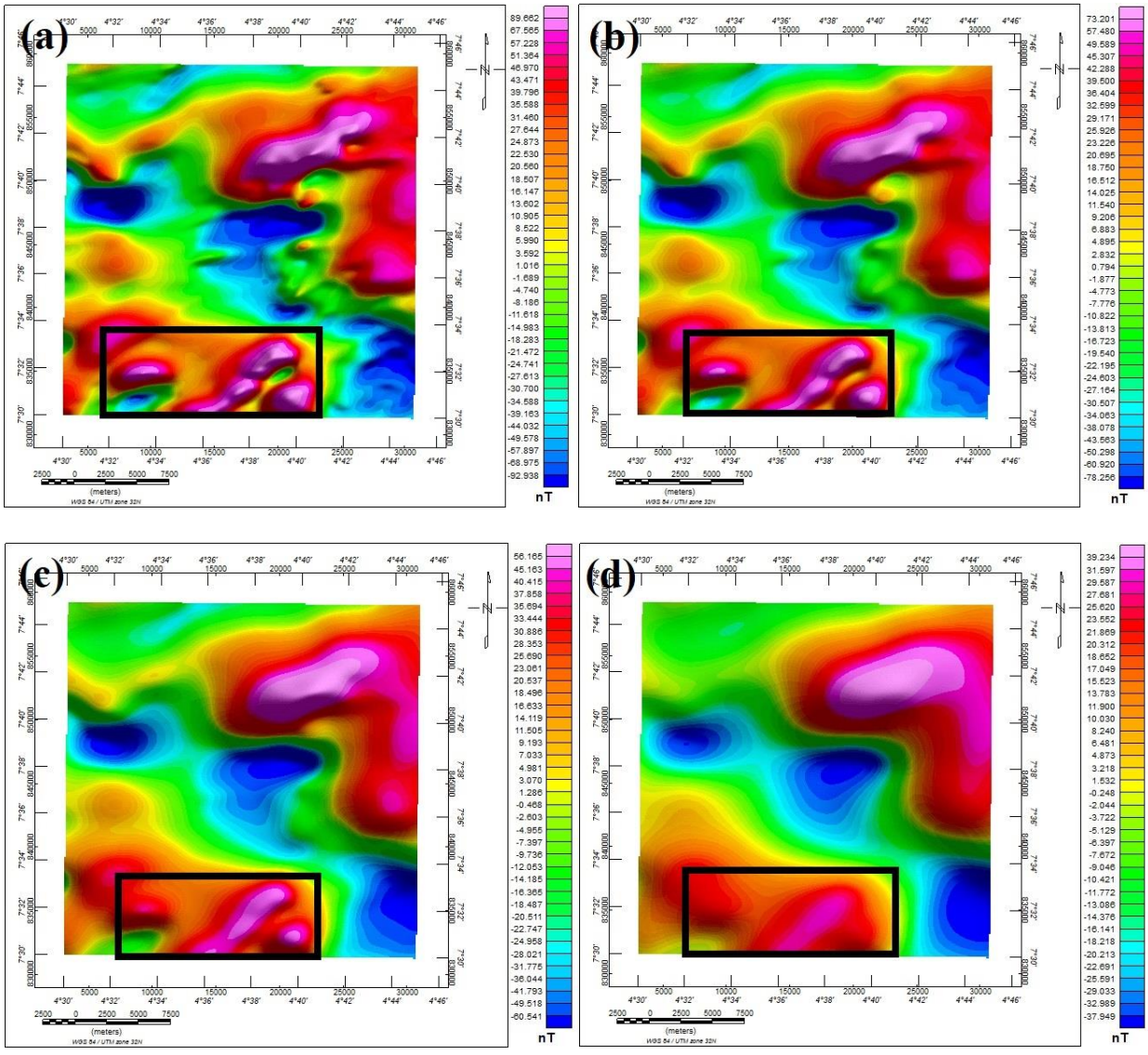

Figure 10 Upward continuation of residual magnetic intensity map to a height of 200 m, 500 m, 1000 m and 2000 m, respectively.

4.7.2. Total horizontal derivative map

The total horizontal derivative (THDR) map of the study area presented in Fig. 11 reveals the amplitude of total horizontal derivative peaking above the boundaries of magnetic structures associated with lithological contacts in the area. The gradients of the map ranged between 0.004 nT/m and 0.148 nT/m, as indicated in Fig. 11.

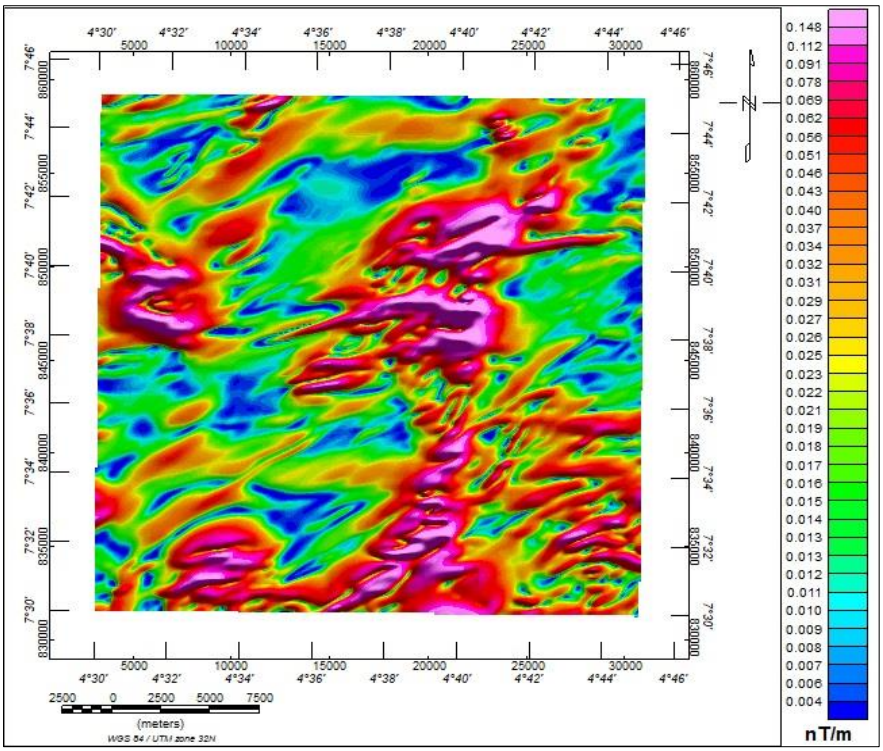

Figure 11 Total horizontal derivative map of the study area

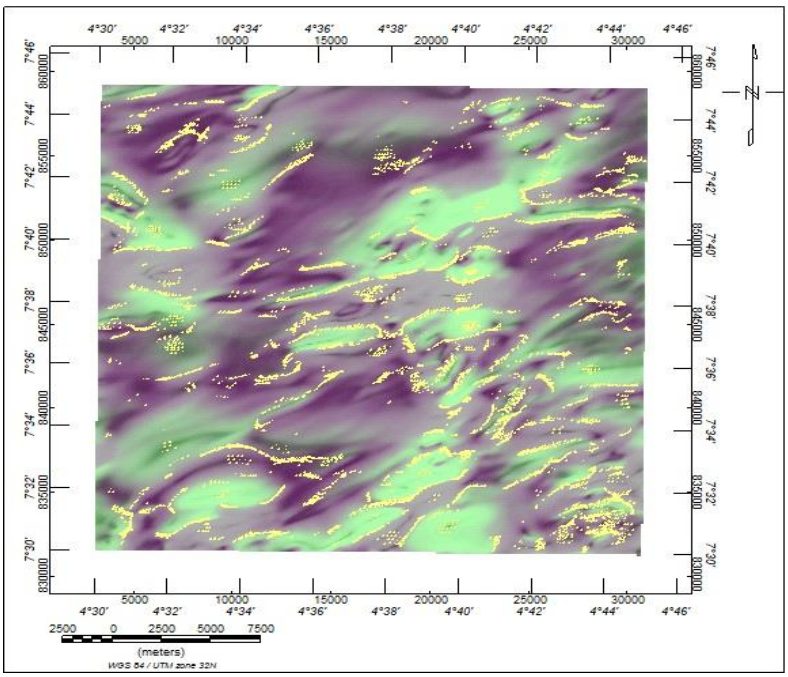

Figure 12 The composite grid of FVD (green), THDR (gray) and ASA (magenta), overlain by 3D ED plots (yellow) with structural index of zero and one

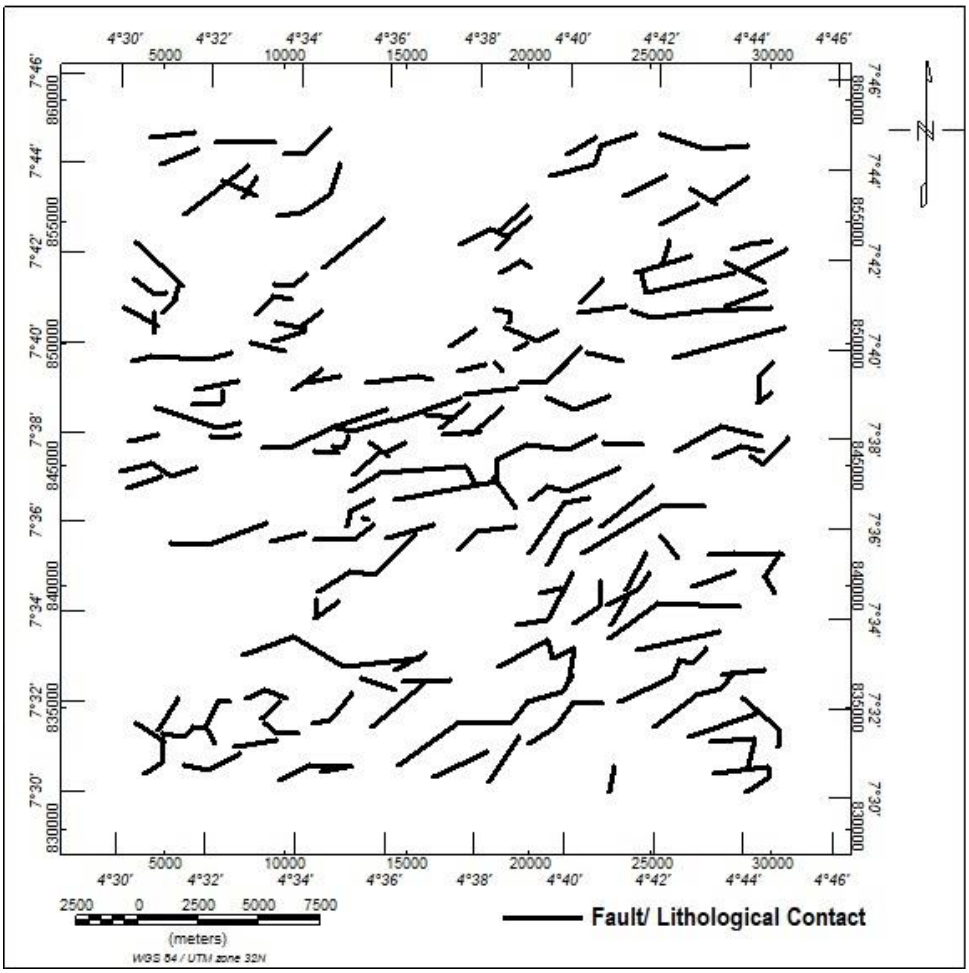

Figure 13 Structural map of the study area

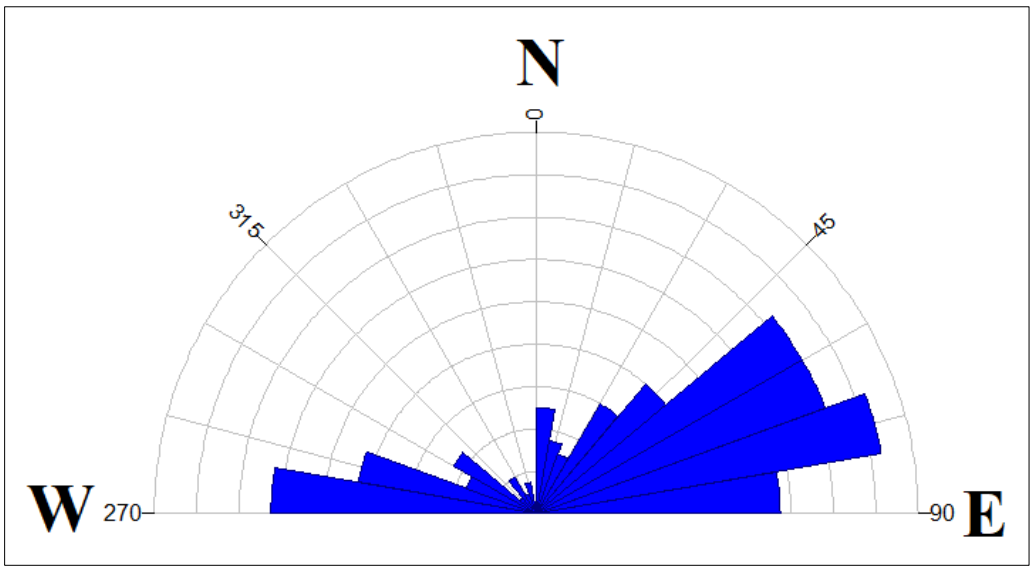

Figure 14 Rose diagram of the extracted magnetic lineaments

The faults and lithological contacts in the study area were delineated using composite maps involving first vertical derivative, total horizontal derivative, analytical signal amplitude overlain by 3D Euler deconvolution plots as presented in Fig. 12. These identified structural discontinuities (magnetic lineaments) are subsequently presented as structural map as indicated in Fig. 13. The observed high lineament density in the area is an indication of good groundwater prospect, most especially the locations underlain by lineament intersections. The visual comparison of the faults/ lithological boundaries in the study area with Ifewara faults system revealed evidence of related deformation in the basement framework as suggested by the northeast to southwest trending structural discontinuities. The Rose diagram (Fig. 14) also depicted the orientations of the extracted lineaments as E-W, NE-SW, WWN-EES, N-S, WWS-EEN and SSW-NNE; which is an indication of complexity in structural geology of the study area. The northeast-southeast alignment is associated with Pan African orogeny, the northwest-southeast direction represent Kibarian orogeny while the east-west trend is an indication of Liberian orogeny [33].

5. Conclusion

The possible zones of structural discontinuities in the study area have been successfully investigated through the application of edge detection methods involving analytical signal magnitude, first vertical derivative, total horizontal derivative and 3D Euler deconvolution plots. The lineament intersection density observed in the area suggests good aquifer zones with high groundwater prospects. The analysis of the rose diagram revealed the delineated structural discontinuities trend majorly towards the NE-SW direction. These structural anomalies in the basement fabrics are suggestive of crustal stress similar to Ifewara fault networks; indicative of future possible events of earthquake hazard in the area. Furthermore, the calculated depth to magnetic basement ranged between 55 m and 345 m, 13 m and 250 m and 142 and 1389 m as indicated in the Euler deconvolution, spectral analysis and source parameter imaging maps, respectively. It is however recommended that further geophysical studies involving electrical and seismic refraction methods should be carried out to confirm the groundwater potential as well as fracture distribution and their depths of occurrence at the subsurface within the area.

Compliance with ethical standards

Acknowledgments

The authors are grateful to the Nigerian Geological Survey Agency for making aeromagnetic data available at low cost.

Disclosure of conflict of interest

No conflict of interest was reported by any of the authors.

References

[1] Olurin OT. Interpretation of high resolution airborne magnetic data (HRAMD) of Ilesha and its environs, Southwest Nigeria, using Euler deconvolution method. Original Scientifc Paper. 2017; doi 10.1515/rmzmag-2017-0013.

[2] Milson J. Field Geophysics. England: John Wiley & Sons. 2003; 249 p.

[3] Reeves C. Aeromagnetic Surveys: principle, practice and interpretation. Geosoft INC. 2007; 155 p.

[4] Elueze AA. Petrology and gold mineralization of the amphibolites belt. Ilesa area southwestern Nigeria. Geo. Mijnb. 1986; 65: 189-195.

[5] Folami SL. Interpretation of aeromagnetic anomalies in Iwaraja area, southwestern Nigeria. J. Min. Geol. 1992; 28 (2): 391-396.

[6] Kayode JS. Ground magnetic study of Jeda-iloko area, southwestern Nigeria and its geological implications. Department of Applied Geophysics, Federal University of Technology, Akure, M.tech (2006).

[7] Akinlalu AA, Adelusi AO, Olayanju GM, Adiat KAN, Omosuyi GO, Anifowose AYB, Akeredolu BE. Aeromagnetic mapping of basement structures and mineralization characterisation of Ilesa Schist Belt, Southwestern Nigeria. Journal of African Earth Sciences. 2018; 138: 383-391.

[8] Hubbard FH. Precambrian crustal development in western Nigeria: indications from the Iwo region. Geological Society of America Bulletin. 1975; 20(1): 117-139.

[9] Ajibade AC. The nigerian precambrian and the Pan-African orogeny. In: The precambrian geology of Nigeria (P.O. Oluyide et al., eds); Proceedings of the first symposium on the precambrian geology of Nigeria, Geological Survey of Nigeria. 1979; pp. 45-53.

[10] Rahaman MA. Recent advances in the study of the basement complex of Nigeria. Symposium on the geology of Nigeria. Obafemi Awolowo University, Nigeria (1988).

[11] Dada SS. Proterozoic evolution of Nigeria. In: Oshi O. (ed) The basement complex of Nigeria and its mineral resources. Akin Jinad & Co, Ibadan. 2006; pp 29–44.

[12] Ferre E, De le ris J, Bouchez JL, Lar AU, Peucat JJ. The Pan-African Reactivation of Contrasted Eburnean and Archaean Provinces in Nigeria: Structural and Isotopic Data, vol. 153. Journal of the Geological Society, London. 1996; pp. 719-728.

[13] Ajibade AC. The cataclastic rocks of the Zungeru region and tectonic significance. J. Min. Geol. 1982; 18: 29-41.

[14] Adeoti B, Okonkwo CT. Structural evolution of Iwaraja shear zone, southwestern Nigeria. J. Afr. Earth Sci. 2017; 131: 117-127.

[15] Odeyemi IB. A comparative study of remote sensing images of the structure of okemesi fold belt, Nigeria. ITC J. 1993; 1: 77-81.

[16] Okonkwo CT, Adetunji A, Folorunso IO. "Microstructural and mineralogical evolution of the oke awon shear zone in the jebba area, southwestern Nigeria. Pac. J. Sci. Technol. 2014; 15: 335-344.

[17] Odeyemi IB. A review of the orogenic events in the basement complex of Nigeria, West Africa. Geol. Rundsch. 1981; 70 (3): 897-909.

[18] Ademeso OA, Adekoya JA, Adetunji A. "Further evidence of cataclasis in the Ife-Ilesa schist belt, southwestern." Nigeria. J. Nat. Sci. Res. 2013; 3 (11), 50-59.

[19] Obaje NG. Geology and mineral resources of Nigeria. Springer, Dordrecht Heidelberg London New York. 2009; 221 p.

[20] Awoyemi MO, Ajama OD, Hammed OS, Arogundade AB, Falade SC. Geophysical mapping of buried faults in parts of Bida Basin, North Central Nigeria. European Association of Geoscientists & Engineers, Geophysical Prospecting. 2017; 1–15.

[21] Reeves C. Aeromagnetic Surveys: Principles, Practice & Interpretation. Geosoft. 2005; pp. 104, 140.

[22] MacLeod IN, Jones K, Dai TF. 3-D analytic signal in the interpretation of total magnetic field data at low magnetic latitudes. Exploration Geophysics. 1993; 24: 679–688.

[23] Jeng Y, Lee YL, Chen CY, Lin MJ. Integrated Signal Enhancements in Magnetic Investigation in Archaeology. Journal of Applied Geophysics. 2003; 53: 31–48.

[24] Reid AB, Allsop JM, Granser H, Millet AJ, Somerton IW. Magnetic interpretation in three dimensions using Euler deconvolution. Geophysics. 1990; 55: 80–91.

[25] Thompson DT. EULDPH: a new technique for making computer assisted depth estimates from magnetic data. Geophysics. 1982; 47: 31–37.

[26] Spector A, Grant FS. Statistical Models for interpreting aeromagnetic data. Geophysics. 1970; 35: 293-302.

[27] Lee YW. Statistical theory of communication. Wiley, New York. 1960; pp 1-75.

[28] Thurston JB, Smith RS. Automatic conversion of magnetic data to depth, dip, and susceptibility contrast using the SPI (TM) method. Geophysics. 1997; 62: 807-813.

[29] Thurston JB, Guillon JC, Smith RS. Model-independent depth estimation with the SPITM method: SEG Expand Abstracts. 1999; 18: 403-406.

[30] Smith RS, Thurston JB, Dai T, MacLeod IN. iSPITM- the improved source parameter imaging method. Geophysical Prospecting. 1998; 46: 141-151.

[31] Nabighian MN, Ander R, Grauch VJS, Hansen RO, LaFehr T, Li Y, Pearson WC, Pierce JW, Phillips JD, Ruder ME. The historical development of the gravity method in exploration: Geophysics. 2005; 70: 63-89.

[32] Odeyemi IB. Lithostratigraphy and structural relationships of the upper precambrian metasediments Igarra area, southwestern Nigeria. In: Oluyide PO, Mbonu WC, Ogezi AE, Egbiniwe IG, Ajibade AC, Umeji AC (Eds.). Precambrian Geology of Nigeria. Geological Survey of Nigeria. 1988; pp. 111-125.